Academic Journal of Science and Technology
ISSN: 2771-3032 | Vol. 5, No. 3, 2023

Research on Alpine Glacier Deformation Monitoring Based on D-InSAR

Xin Gao

School of Surveying, Mapping and Land Information Engineering, Henan Polytechnic University, Jiaozuo 454000, Henan, China

Abstract: Using Sentinel-1A data in 2021, the displacement of Tomur Glacier in the radar line of sight is obtained by repeated orbit differential interferometry. By introducing ice flow factor and combining glacier slope, the vertical deformation is extracted as the surface elevation change. The results of the study found that the overall average annual elevation change of Tomur Glacier decreased by -14.03m, with an average decrease of -0.26 $\mathrm{m}\cdot a^{-1}$. The reliability of the model was verified, and the results of the comparative study revealed that the glacier thinning rate has been increasing in recent years, and the trend of glacier retreat is becoming more severe.

Keywords: Sentinel-1A, Ice flow factor, Glacier surface elevation change, Slope.

1. Introduction

Glacier monitoring has always been an important part of glaciological research, and glacier surface elevation measurements are an important part of glacier monitoring research. Glacier surface elevation monitoring is also known as glacier thickness change monitoring[1]. The traditional measurement method mainly uses spline data to calculate glacier thickness change. Due to the difficulty and danger of obtaining data from traditional field monitoring, it plays a very limiting role in studying glacier changes[2]. With the rapid development of remote sensing technology and the application of 3S technology in the cryosphere, remote sensing monitoring has become a key tool for rapid acquisition of glacier changes. In 2002, Strozzi[3] obtained the change field of glacier motion in northern Svalbard based on offset tracking method, which confirmed that the offset tracking method could be used to obtain the information of glacier motion. Domestic scholars Zhou[4] used the D-InSAR technique for the first time in winter on the Dungkemadi glacier and obtained information on glacier thickness changes over a few days interval, demonstrating the feasibility of the D-InSAR technique in the study of monitoring thickness changes of mountain glaciers over short-term intervals. Vijay[5] obtained the changes in glacial material balance within the study area from 2000-2012 based on SRTM C/X DEM, TanDEM-X data by correcting for the difference in penetration between SRTM DEM C-band and X-band. When monitoring alpine glaciers, due to their undulating terrain, most of the observed images are covered by clouds and fog.

Based on the two-track DInSAR method, this paper firstly obtains the deformation of the Tomer glacier in the LOS direction, extracts the glacier vertical change by combining the glacier slope, and compares it with the level monitoring results as the glacier elevation change, verifying the reliability of the model. It provides a reliable way to study surface elevation change in alpine glaciers.

2. Principle and Method

2.1. Relationship between LOS-oriented deformation and 3D deformation vectors

The principle of synthetic aperture radar (SAR) imaging by side view is shown in Figure 1. A spatially right-angled coordinate frame is constructed with the subsatellite point of the satellite at the moment of imaging as the coordinate origin O, with eastward, northward and vertical orientations. S is the satellite position at the moment of imaging; P is the ground point, the line between S and P is the radar line of sight (LOS) direction, the angle θ between the LOS direction and the vertical direction is the angle of incidence of the radar signal, and the under star point trajectory is the projection of the satellite orbit on the horizontal plane. φ is the satellite heading angle, The line between the point O under the star and the target point P is the projection of the LOS onto the horizontal plane. Looking at Figure 1 it can be seen that the LOS vector deformation D at point P is the sum of the projections of the 3D displacement components of the point upwards in LOS.

$$\mathrm{D} = D_v \cos\theta + D_n \sin\varphi \sin\theta - D_e \cos\varphi \sin\theta \quad (1)$$

$$\mathrm{D} = D_v \cos\theta + D_n \sin\varphi \sin\theta - D_e \cos\varphi \sin\theta \quad (2)$$

Where D_e is the deformation component of point P along the east-west direction; D_n is the deformation component of point P along the north-south direction; D_v is the deformation component of point P along the vertical direction.

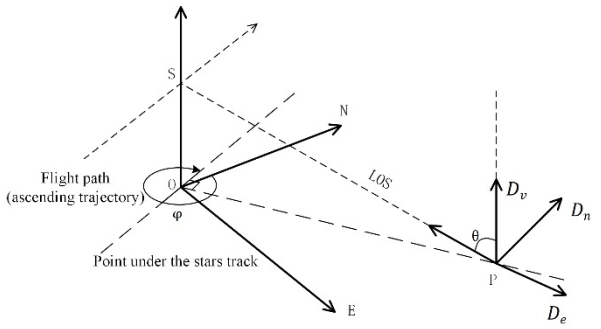

Figure 1. SAR side-view imaging geometry and angular parameters

2.2. Determination of the ice flow direction factor

The ice flow slope inclination angle α is replaced using the average ice surface slope value. The slope is calculated as follows: first the downloaded elevation data is converted to raster form, assuming a 3*3 window area with an elevation difference of H and a horizontal distance of M. The slope L is calculated using the formula: $L = (H/M) * 100\%$,or $\tan L = H/M$.

The direction of ice flow generally follows the direction of greatest slope downwards within a certain range or along the glacier midline, parallel to the flanks, leaving ice flow traces in areas where the glacier movement is regular and stable. In practice, the ice flow movement is complex. In this paper, the subsequent determination of the ice flow direction will be combined with the elevation of the study area, optical images and topographic features, and a variety of methods will be considered to determine the ice flow direction.

3. Experiments and Results

3.1. Study Area Overview

The Tomur Peak area is located in the westernmost tip of the Tianshan Mountains in China, the southern foot of the Tianshan Mountains, and the northern margin of the Tarim Basin. It is basically composed of four mountains, namely the east-west Halazhouliha Mountain, the Hantenggeli Mountain, the Tomur Mountain and the north-south Ziwu Mountain. The average altitude of the mountains is 5400-6600 m, with the highest peak of the Tianshan Mountains, Tomur Peak (7435.3m)[6]. Among them, glaciers less than or equal to 5km2 account for 85 %, and the types are valley glaciers and suspended glaciers. The precipitation in this area is mainly supplied by the moist airflow from the Atlantic and Arctic oceans. The location of Tomur Glacier is shown in Fig.2.

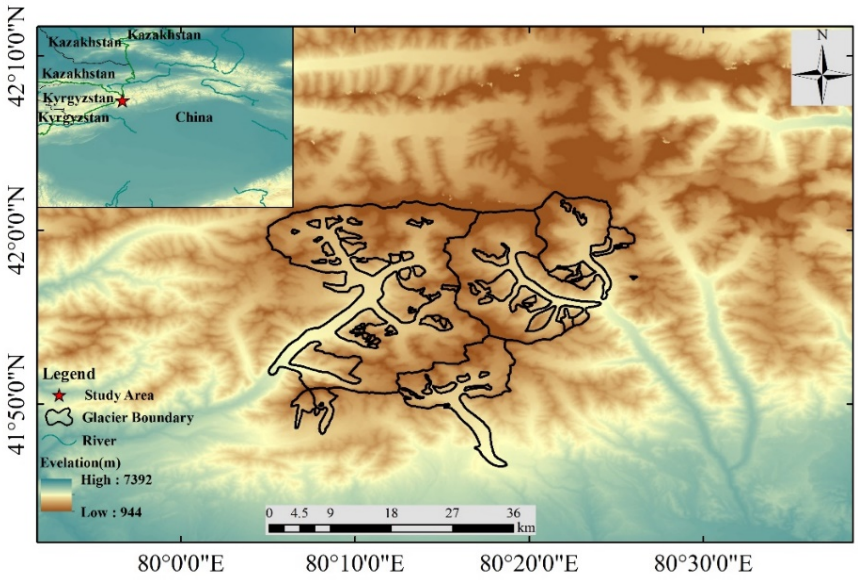

Figure 2. Overview of the study area

3.2. Data source

The SAR image experimental data selected in this paper are Sentinel-1A image data on August 16,2021 and September 9,2021. The wavelength of SAR data is 5.63 cm (C band), and the polarization mode is VV polarization. The main image incident angle is 39.394 °, the time baseline is 24 d, and the spatial baseline is 70.707 m[7].

Landsat-7 satellite was launched on April 15, 1999, which is a series of American land exploration satellites. Landsat-7 satellite is equipped with an enhanced thematic mapper (ETM +). Compared with Landsat-5 satellite TM sensors, ETM + has an additional band with a resolution of 15 meters and a higher resolution in the infrared band, so it has higher accuracy[8].

SRTM is a radar topographic mapping mission that began on February 11, 2000 by NASA, the Geospatial-Intelligence Agency, and the space agencies of Germany and Italy. It carried out a total of 222 hours and 23 minutes of data collection for 11 days, and obtained radar image data covering more than 119 million square kilometers between 60 degrees north latitude and 60 degrees south latitude, covering more than 80 % of the Earth 's land surface[9].

The Glacier Cataloging Dataset is from the National Snow and Ice Data Center (http://www.glims.org/RGI/) produced by the RGI and Glacier Monitoring Infrastructure Working Group, an organization of the International Association of Cryosphere Sciences (IACS). The RGI 6.0 (Randolph Glacier Inventory 6.0) database released in July 2017 was used to catalog the glaciers[10].

3.3. Experimental result

A glacier in the Western Tianshan Mountains, Tomur Glacier, was selected as the research object. The three-dimensional information was extracted by the three-dimensional extraction model of the glacier. The geocoded deformation map is shown in Figure 3.

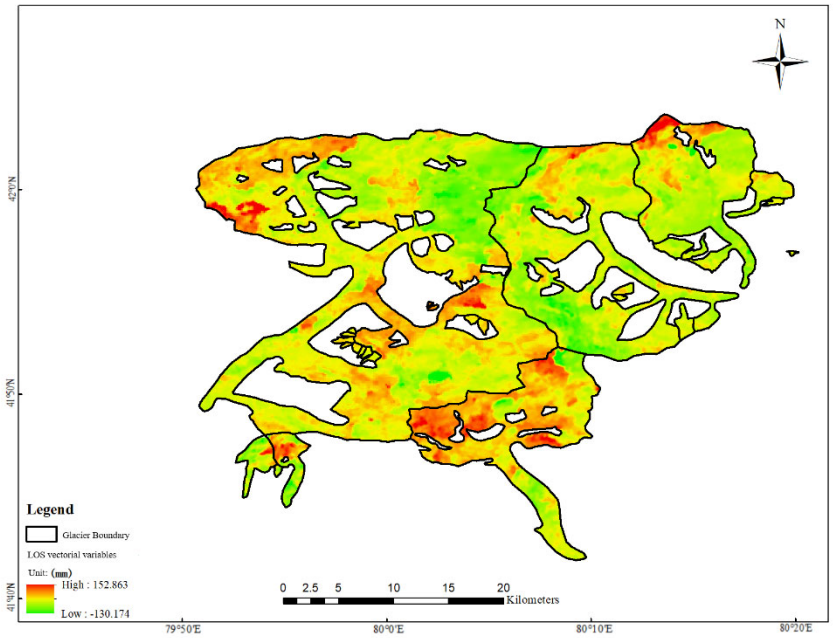

Figure 3. LOS displacement to the line of sight

4. Discussion and Analysis

On the premise that the ice flow direction of Tomur Glacier is known, the feature points are selected, as shown in Fig.4. In order to obtain the observation points with strong reliability, the coherence threshold detection method is used to extract the area with coherence greater than 0.2. the threshold detection, the glacier area with better interference effect can be selected to ensure the reliability of the results to a certain extent.

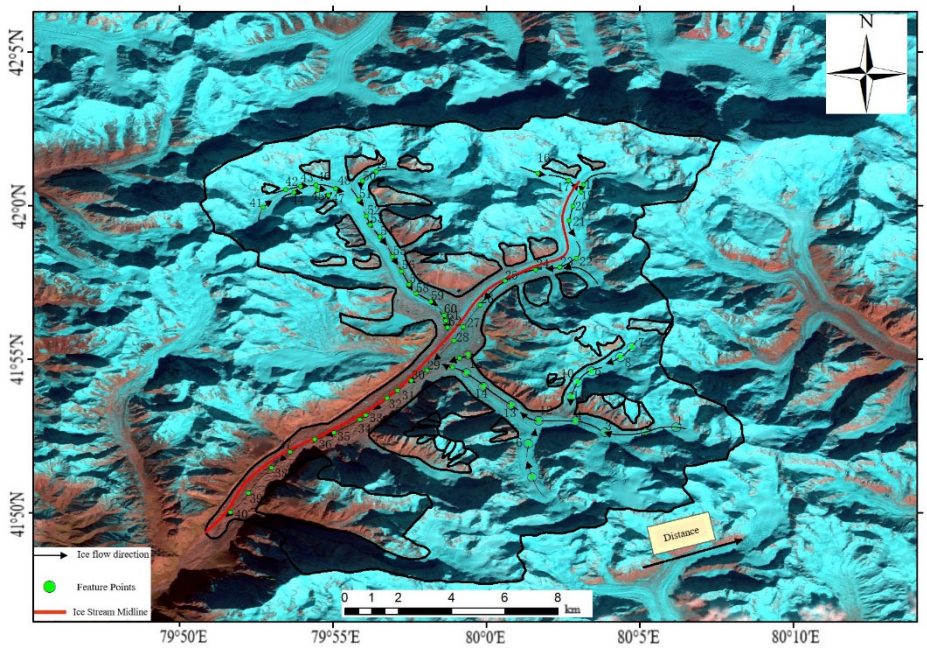

Figure 4. Regional feature point selection diagram

Due to the large slope of feature points more than 40 °, the large slope will have a certain impact on the stability of radar LOS deformation. It is converted into the real change of glacier H, and the calculation formula of H is:

$$H = \frac{\Delta R \cdot 365}{K \cdot 24} \tag{3}$$

On this basis, the annual elevation variation D of glaciers

is calculated. The calculation formula of D is:

The results are shown in Table 1.

$$D = H \cdot \sin\alpha \qquad (4)$$

Table 1. Feature point calculation table

serial	Direction angle of ice flow/β	Ice flow slope angle/α	Δ*R* /mm	K	H m/yr	D m/yr
2	178	22	27	0.49	0.84	-0.14
3	148	34	38	0.84	0.69	0.29
4	163	15	15	-0.5	-0.46	-0.39
5	94	32	6	0.70	0.12	0.07
6	57	37	20	0.97	0.31	-0.07
15	116	18	24	-0.52	-0.71	0.55
16	29	26	2	-0.33	-0.08	-0.08
17	44	30	-12	0.63	-0.29	0.25
20	123	34	-18	0.73	-0.37	-0.17
21	113	30	-21	0.24	-1.35	1.35
30	161	31	23	-0.58	-0.60	0.26
35	173	30	10	0.31	0.44	-0.44
36	177	15	-2	-0.36	0.06	0.05
40	157	22	10	-1	-0.14	-0.01
43	346	24	40	0.50	1.19	-1.08
50	129	20	-11	0.34	-0.48	-0.43
52	79	13	6	-0.88	-0.1	-0.03
59	44	30	17	0.24	1.10	-1.1
60	75	18	11	0.46	0.36	-0.34

5. Conclusion

In this paper, the deformation of Tomur Glacier in LOS direction is obtained by two-track DInSAR. Combined with the variables (ice flow direction angle, ice flow slope angle), The vertical variation is extracted by combining the slope of glacier, and it is used as the result of glacier elevation change. Compared with the leveling monitoring results, it is found that the annual average elevation change of Tomur Glacier decreases by-14.03 m, with an average decrease of-0.26 $\mathrm{m} \cdot a^{-1}$. The comparative study found that the rate of glacier thinning has increased in recent years, indicating that glacier retreat has become more serious.

References

[1] HUBER J, MCNABB R, ZEMP M. Elevation Changes of West-Central Greenland Glaciers From 1985 to 2012 From Remote Sensing [J]. Frontiers in Earth Science, 2020, 8.

[2] KääB A, LEINSS S, GILBERT A, et al. Massive collapse of two glaciers in western Tibet in 2016 after surge-like instability [J]. Nature Geoscience, 2018, 11(2): 114-20.

[3] LUCKMAN A, MURRAY T, STROZZI T. Surface flow evolution throughout a glacier surge measured by satellite radar interferometry [J]. Geophysical Research Letters, 2002, 29(23): 10-1--4.

[4] ZHOU Jianmin , LI Zhen, LI Xinwu Method for extracting glacial topography and movement velocity from Qinghai-Tibet Plateau based on ERS tandem interference data[J]. High Technology Communications, 2009, 19(09): 964-70

[5] VIJAY S, BRAUN M. Elevation Change Rates of Glaciers in the Lahaul-Spiti (Western Himalaya, India) during 2000–2012 and 2012–2013 [J]. Remote Sensing, 2016, 8(12).

[6] KANG Ersi, ZHU Shousen, HUANG Mingmin Glacial hydrology in the Tomur Peak area[J]. Journal of Glaciology and Geocryology, 1980, (04): 18-21

[7] AðALGEIRSDóTTIR G, MAGNúSSON E, PáLSSON F, et al. Glacier Changes in Iceland From ~1890 to 2019 [J]. Frontiers in Earth Science, 2020, 8.

[8] MUHAMMAD S, TIAN L, KHAN A. Early twenty-first century glacier mass losses in the Indus Basin constrained by density assumptions [J]. Journal of Hydrology, 2019, 574: 467-75.

[9] WENDLEDER A, FELBIER A, WESSEL B, et al. A Method to Estimate Long-Wave Height Errors of SRTM C-Band DEM [J]. IEEE Geoscience and Remote Sensing Letters, 2016, 13(5): 696-700.

[10] SUN Y, JIANG L, LIU L, et al. Mapping Glacier Elevations and Their Changes in the Western Qilian Mountains, Northern Tibetan Plateau, by Bistatic InSAR [J]. IEEE Journal of Selected Topics in Applied Earth Observations and Remote Sensing, 2017: 1-11.